About OMICS Group

OMICS Group International is an amalgamation of Open Access publications and worldwide international science conferences and events. Established in the year 2007 with the sole aim of making the information on Sciences and technology 'Open Access', OMICS Group publishes 400 online open access scholarly journals in all aspects of Science, Engineering, Management and Technology journals. OMICS Group has been instrumental in taking the knowledge on Science & technology to the doorsteps of ordinary men and women. Research Scholars, Students, Libraries, Educational Institutions, Research centers and the industry are main stakeholders that benefitted greatly from this knowledge dissemination. OMICS Group also organizes 300 International conferences annually across the globe, where knowledge transfer takes place through debates, round table discussions, poster presentations, workshops, symposia and exhibitions.

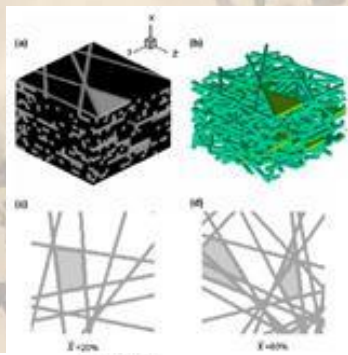
About OMICS Group Conferences

OMICS Group International is a pioneer and leading science event organizer, which publishes around 400 open access journals and conducts over 300 Medical, Clinical, Engineering, Life Sciences, Pharma scientific conferences all over the globe annually with the support of more than 1000 scientific associations and 30,000 editorial board members and 3.5 million followers to its credit.

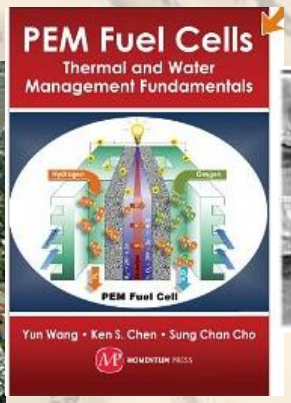
OMICS Group has organized 500 conferences, workshops and national symposiums across the major cities including San Francisco, Las Vegas, San Antonio, Omaha, Orlando, Raleigh, Santa Clara, Chicago, Philadelphia, Baltimore, United Kingdom, Valencia, Dubai, Beijing, Hyderabad, Bengaluru and Mumbai.

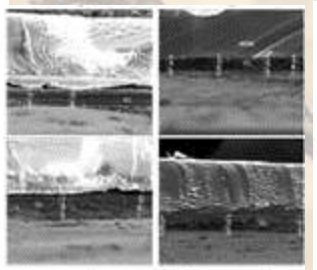
Insoluble Discharge Formation in the Air Cathode of Li-Air Batteries

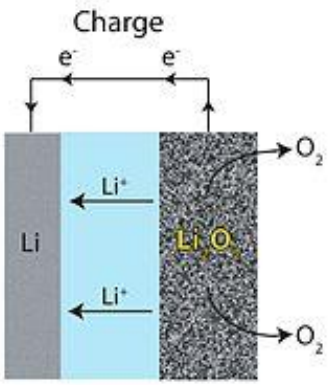
Prof.Yun Wang, Hao Yuan, and Dr. Sun Chan Cho
Renewable Energy Resources Lab
Department of Mechanical & Aerospace Engineering, UC Irvine











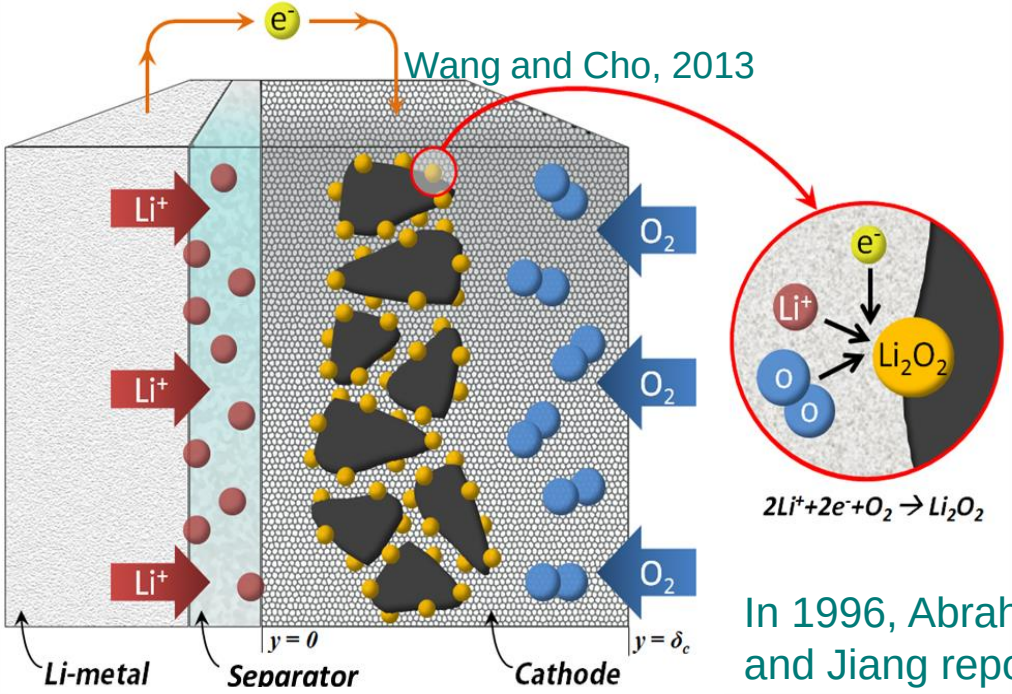
Oct. 6, 2015

UC Irvine: 1965-2015: #39 in US News Ranking 2016.

Outline

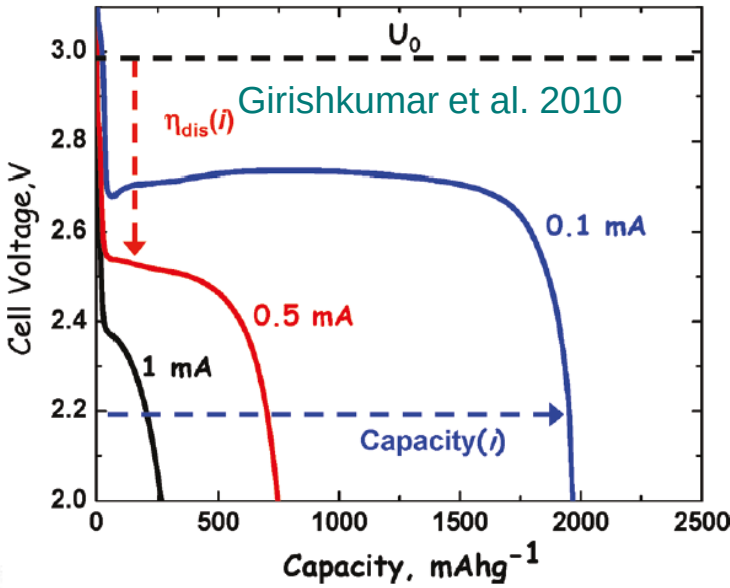
- Introduction to Li-air Battery
- Insoluble Discharge Product Formation
- Li-air Battery V.S. PEM Fuel Cell
- Growth Modes at Reaction Surface
- Analysis of Li-air Battery Performance
- Advanced Multi-dimensional Modeling
- Other Ongoing Work @ the Lab
- Conclusions

Introduction: Li-Air Battery



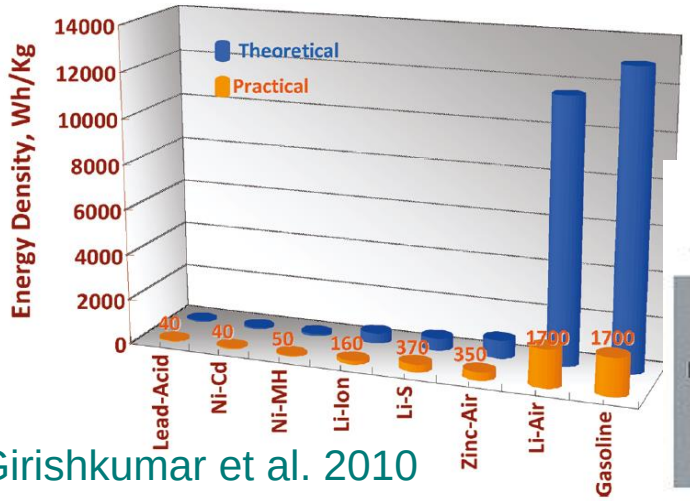
Wang and Cho, 2013

Li-Air Batteries use the oxidation of lithium at the anode and reduction of oxygen at the cathode to induce a current flow. They offer a high theoretical specific energy (11,680 Wh/kg) that is comparable to gasoline (13,000 Wh/kg).

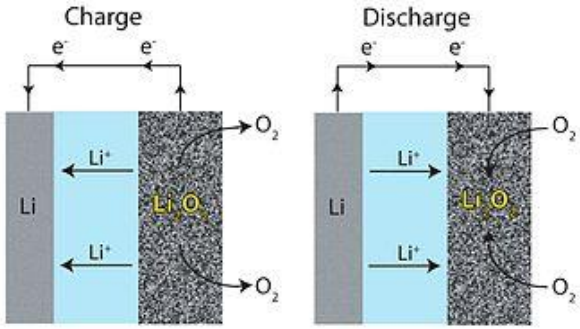


Girishkumar et al. 2010

In 1996, Abraham and Jiang reported the first non-aqueous Li-air batteries that exhibit rechargibility.



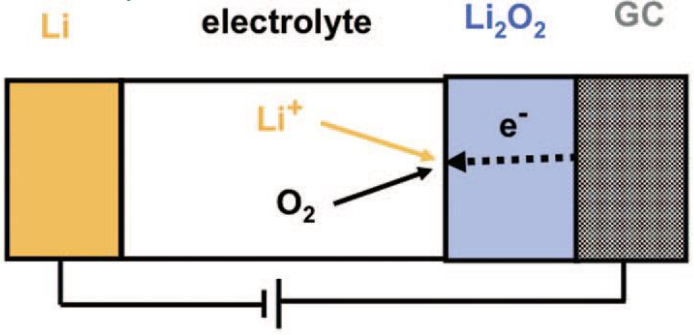
Girishkumar et al. 2010



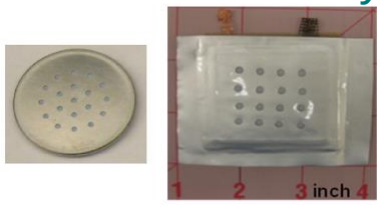
One major issue: practical specific energy is low; low rechargibilty. Capability loss occurs during operation, particular under high current density. One major reason comes from insoluble discharge products formation.

Insoluble Discharge Product Formation

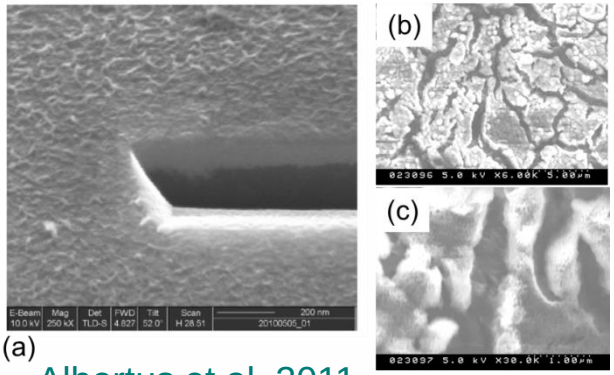
Insoluble product covers the reaction surface; it is low in electric conductivity



Small li-air battery

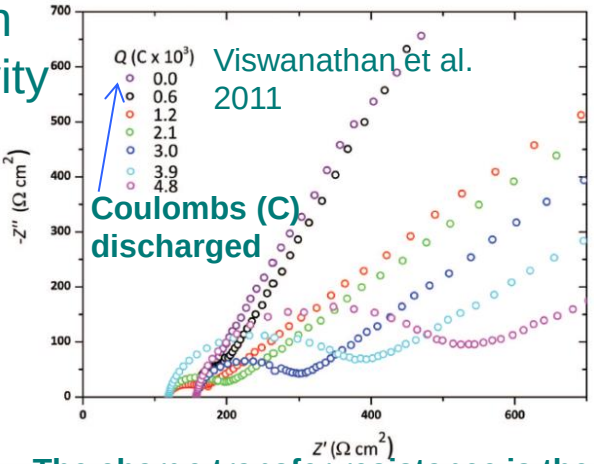


Zhang et al. 2010



Albertus et al. 2011

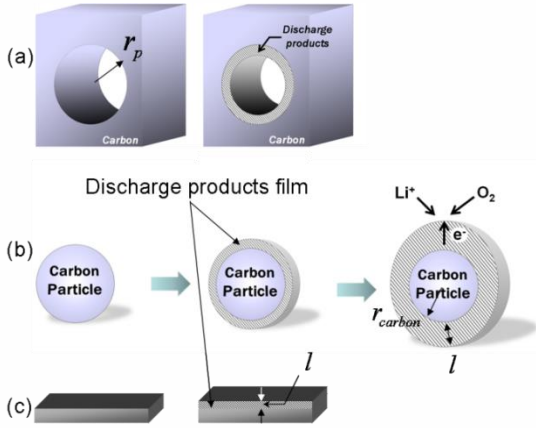
Read and Wang, 2013



Viswanathan et al. 2011

Coulombs (C) discharged

The charge transfer resistance is the semicircle diameter

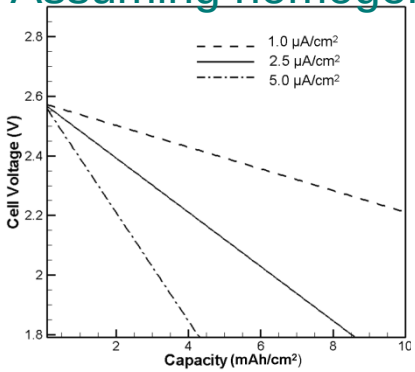


Three typical growth modes

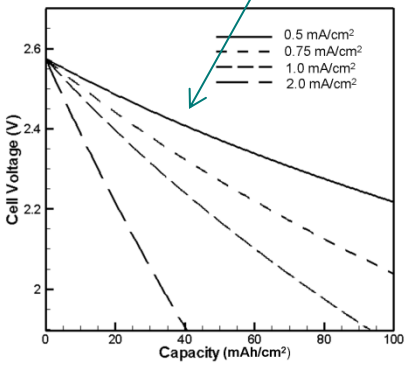
$$\Delta\eta = \frac{I}{a}\left(A_0\left[\sqrt[1/3]{1+\frac{QM_{prod}}{\varepsilon_{carbon}nF\delta_c\rho_{prod}}}-1\right]r_{carbon}+R_0\right)$$

$$\Delta\eta = -\frac{I}{a}\left(A_0\left[1-\sqrt{1-\frac{QM_{prod}}{nF\delta_c\rho_{prod}\varepsilon_p}}\right]r_p+R_0\right)$$

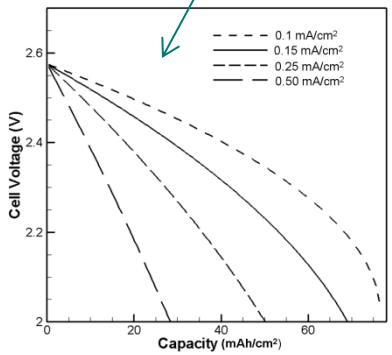
Assuming homogeneous film



planar-film growth mode



spherical-film growth mode

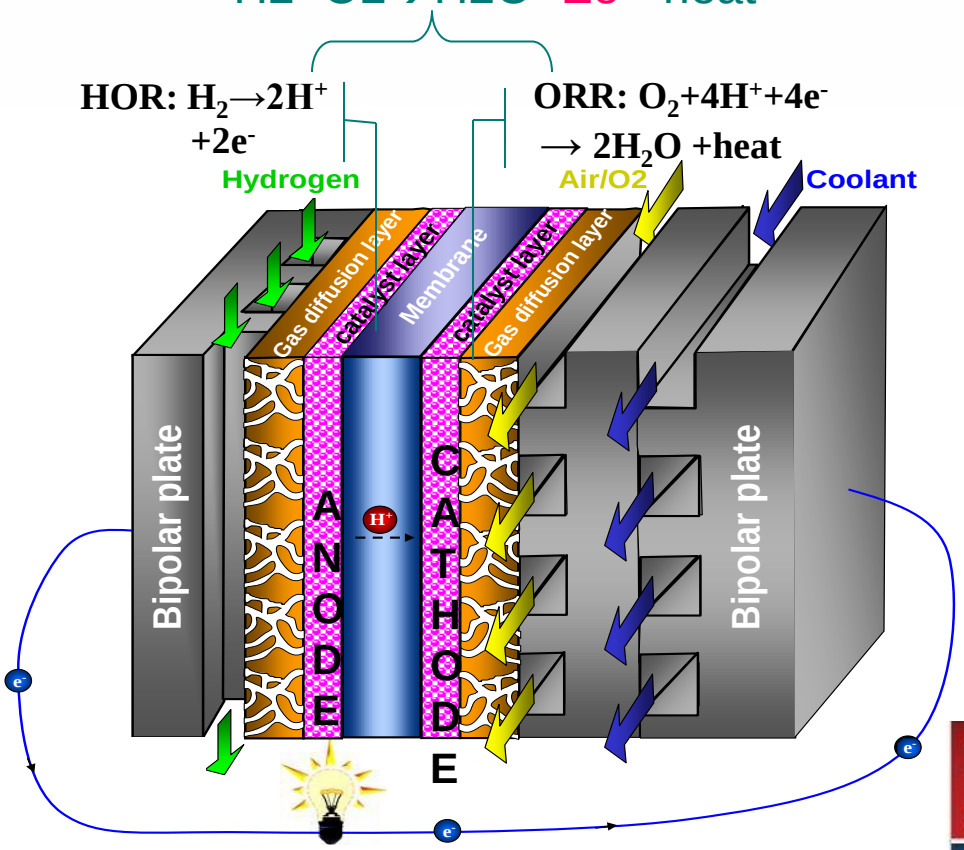


cylindrical-film growth mode

•Y. Wang, Modeling Discharge Deposit Formation and Its Effect on Lithium-air Battery Performance, Electrochimica Acta 75 (2012) 239-246.

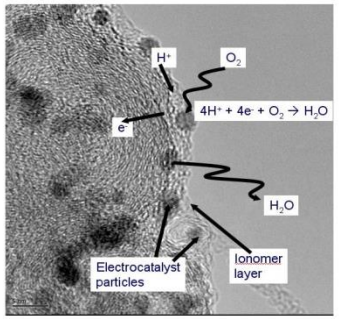
PEM Fuel Cell and Relevance

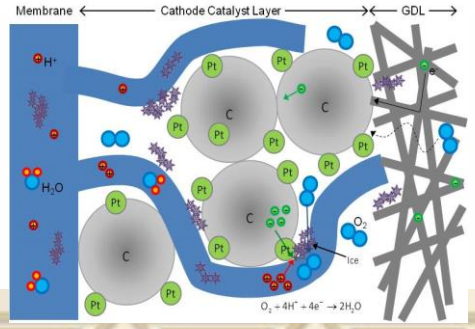
H2+O2→H2O+Ee-+heat

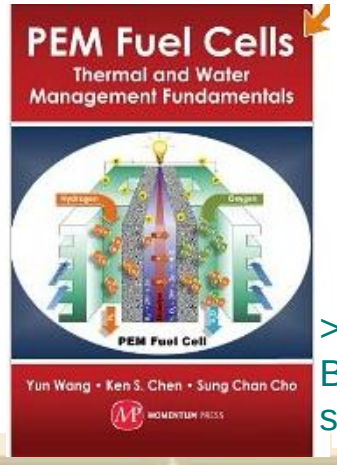


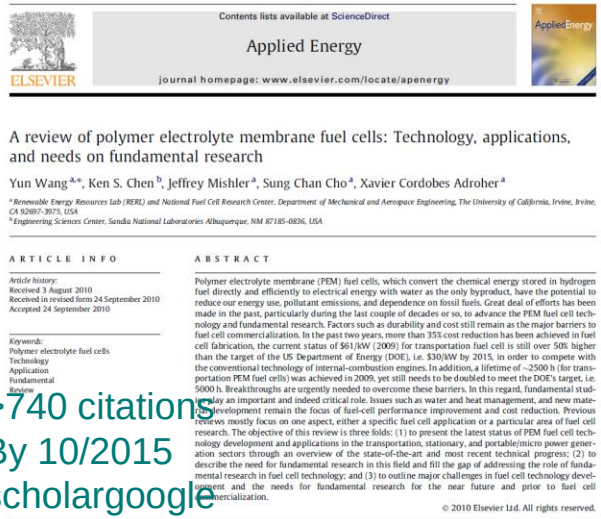
PEFCs, also called PEM (Proton exchange membrane) fuel cells, offer the following **advantages**:

- Primarily use hydrogen & air;
- Only produce water as byproduct;
- High energy capability & efficiency (>50%);
- Operate at low temperature (from -30 to over 100 C°);
- Easy scale-up.



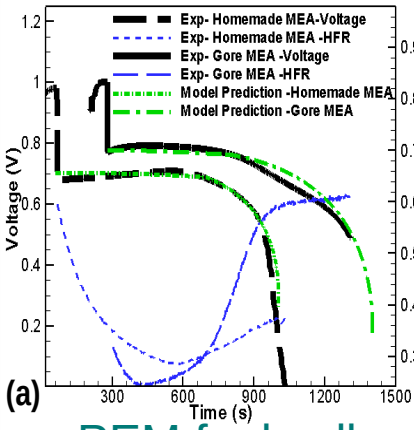




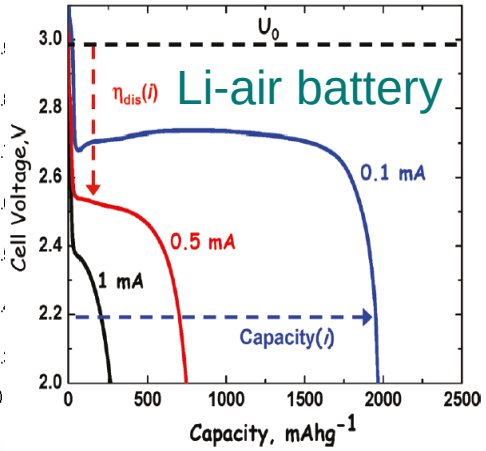


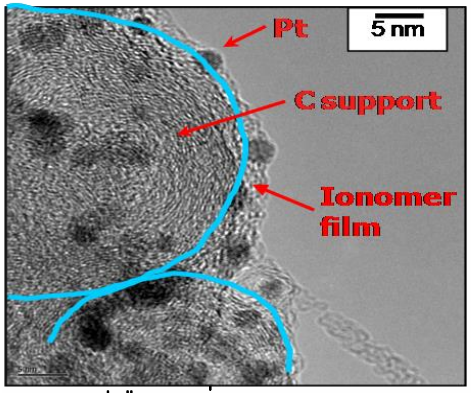
>740 citations By 10/2015 scholargoogle

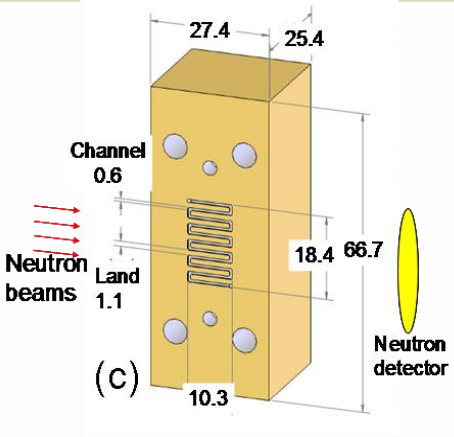
Li-Air Battery V.S. PEM Fuel Cell

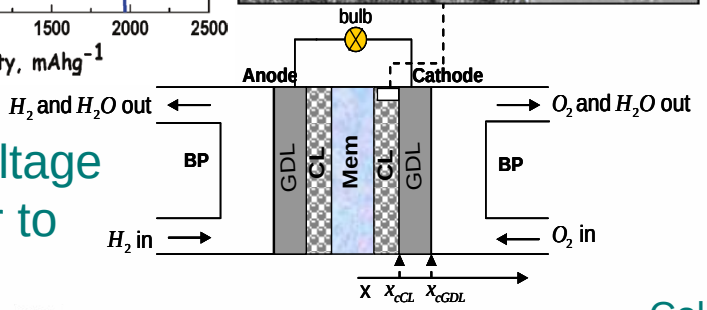


PEM fuel cell



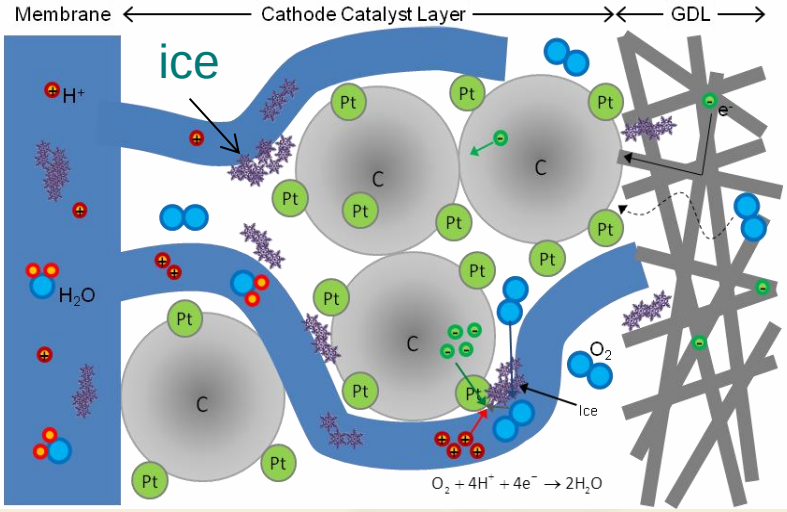


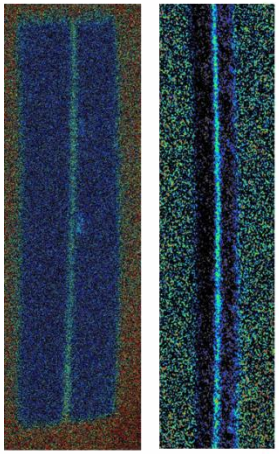




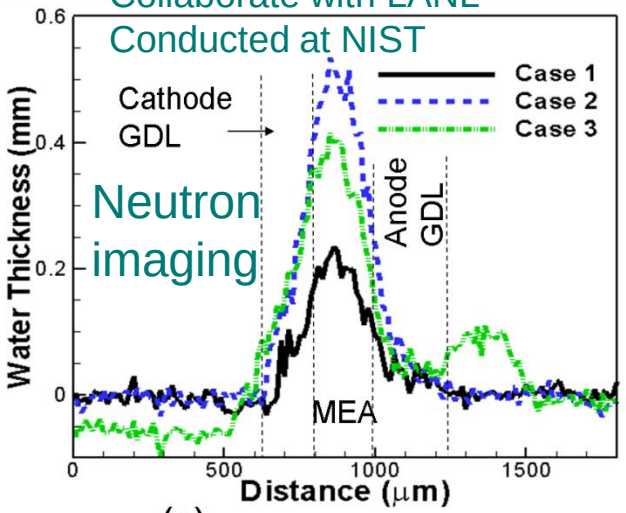
PEM fuel cell shows similar voltage drop due to ice deposit, similar to insoluble product formation.

Product water freezes under sub-freeze temperature, and ice is deposited at local catalyst surface, leading to voltage loss





Collaborate with LANL
Conducted at NIST

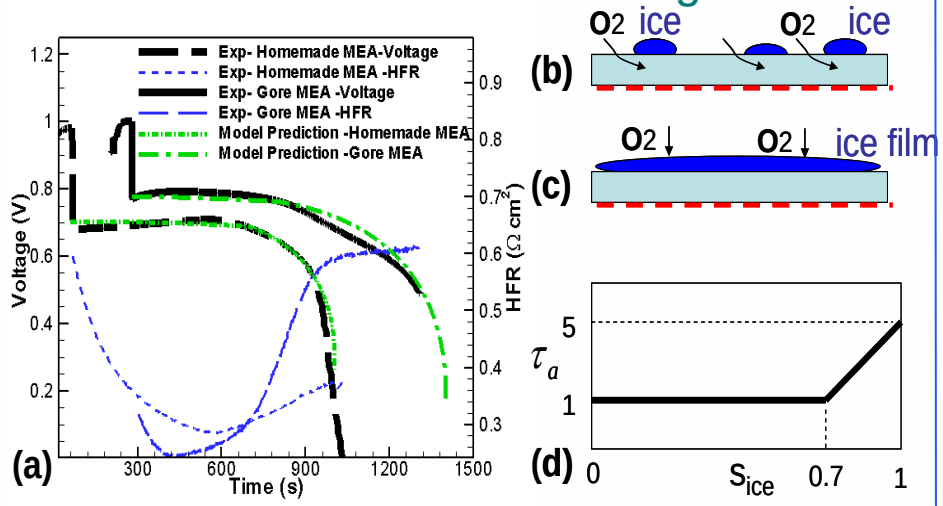


(a) (b) (c)

*Jeff Mishler, Yun Wang, Partha P. Mukherjee, Rangachary Mukundan, and Rodney L. Borup, Subfreezing operation of polymer electrolyte fuel cells: Ice formation and cell performance loss, Electrochimica Acta, 65 (2012) 127-133

Surface Coverage

PEM fuel cell surface coverage



Tafel equation

$$j = -ai_{0,c}^{ref}\frac{C^{O2}}{C^{O2,ref}}\exp\left(-\frac{(1-\beta)F}{RT}\cdot\eta\right)$$

$$= -a_0(1-s_{ice})^{\tau_a} i_{0,c}^{ref}\frac{C^{O2}}{C^{O2,ref}}\exp\left(-\frac{(1-\beta)F}{RT}\cdot\eta\right)$$

Overpotential

$$\eta = -\frac{RT}{\alpha_c F}\ln\left(\frac{IC^{O2,ref}}{a_0 i_{0,c}^{ref}\exp\left[-\frac{E_a}{R}\left(\frac{1}{T_o}-\frac{1}{353.15}\right)\right]C_{cCL}^{O2}\delta_{CL}}\right)$$

$$-\frac{TE_a}{\alpha_c F}\left(\frac{1}{T}-\frac{1}{T_o}\right)+\frac{RT\tau_a}{\alpha_c F}\ln(1-s_{ice})$$

$$+\frac{RT}{\alpha_c F}\ln\left(1-Da\frac{1-\bar{x}^2}{\varepsilon_{CL}^{\tau_d-\tau_{d,0}}(1-s_{ice})^{\tau_d}}\right)$$

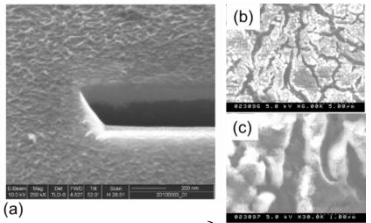
$$= \eta_o + \Delta\eta_T + \Delta\eta_{c,1} + \Delta\eta_{c,2}$$

Battery surface coverage

$$j_c = -a\left(1-\frac{\varepsilon_{prod}}{\varepsilon}\right)^{\tau_a} i_{0,c}^{ref} C_{O2}^{1-\beta} C_{Ce}^{1-\beta}\exp\left(-\frac{1-\beta}{RT}F\eta\right)$$

Overpotential

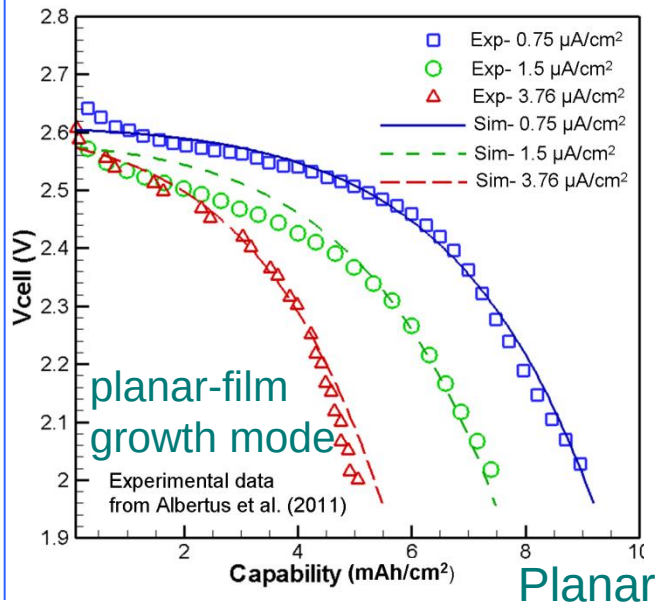
$$\Delta\eta = -\frac{\tau_a RT}{(1-\beta)F}\ln\left(1-\frac{QM_{prod}}{nF\wp_{prod}\delta_c}\right)$$

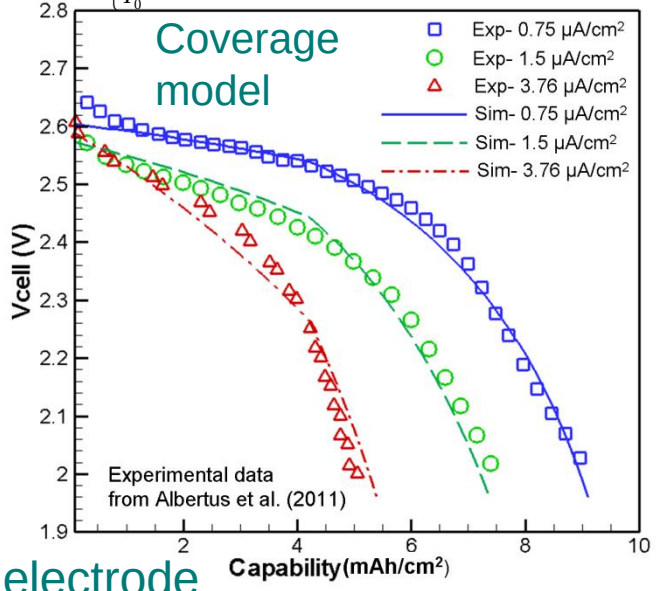


Coverage factor

$$\tau_a = -\frac{I(1-\beta)F}{aRT\ln\left(1-\frac{\varepsilon_{prod}}{\varepsilon}\right)}\left\{A_0\left[\sqrt[1/3]{1-\frac{\varepsilon_{prod}}{\varepsilon_{carbon}}}-1\right]r_{carbon}+R_0\right\}$$

$$\tau_a = \begin{cases} B_1\dfrac{I}{I_0} & s < s_0 \quad \text{where } s = \dfrac{\varepsilon_{prod}}{\varepsilon} \\ \dfrac{I}{I_0}\left(B_1 + B_2(s-s_0)\right) & \text{otherwise} \end{cases}$$

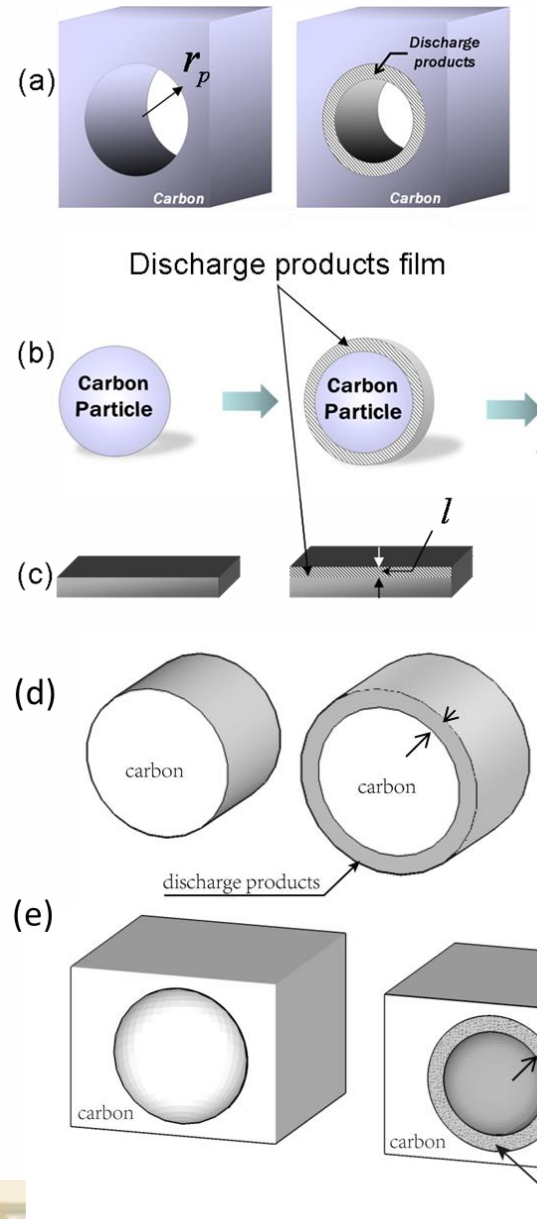




Planar electrode

•Y. Wang, Modeling Discharge Deposit Formation and Its Effect on Lithium-air Battery Performance, Electrochimica Acta 75 (2012) 239-246.

Growth Modes @ Reaction Surface



From a resistor model of the highly-resistive film, the spherical model gives:

$$\tau_a = -\frac{I(1-\beta)F}{a_0 RT \ln\left(1-\frac{\varepsilon_{prod}}{\varepsilon_0}\right)}\left\{A_0\left[\sqrt[1/3]{1+\frac{\varepsilon_{prod}}{\varepsilon_{carbon}}}-1\right]r_{carbon}+R_0\right\}$$

For approximation at s→0 and slope at s0:

$$\tau_a = \begin{cases} B_1\dfrac{I}{I_0} & s < s_0 \quad \text{where} \quad s = \dfrac{\varepsilon_{prod}}{\varepsilon_0} \\ \dfrac{I}{I_0}\left[B_1 + B_2(s-s_0)\right] & \text{otherwise} \end{cases}$$

$$B_1 = \frac{(1-\beta)FA_0 r_{carbon}\varepsilon_0 I_0}{3a_0 RT\varepsilon_{carbon}} \quad \text{and} \quad B_2 = \frac{(1-\beta)FA_0 r_{carbon} I_0}{a_0 RT}\left(\frac{\varepsilon_0/\varepsilon_{carbon}}{3\ln(1-s_0)\left(\frac{s_0\varepsilon_0}{\varepsilon_{carbon}}+1\right)^{2/3}} + \frac{(s_0\varepsilon_0/\varepsilon_{carbon}+1)^{1/3}-1}{(1-s_0)(\ln(1-s_0))^2}\right)$$

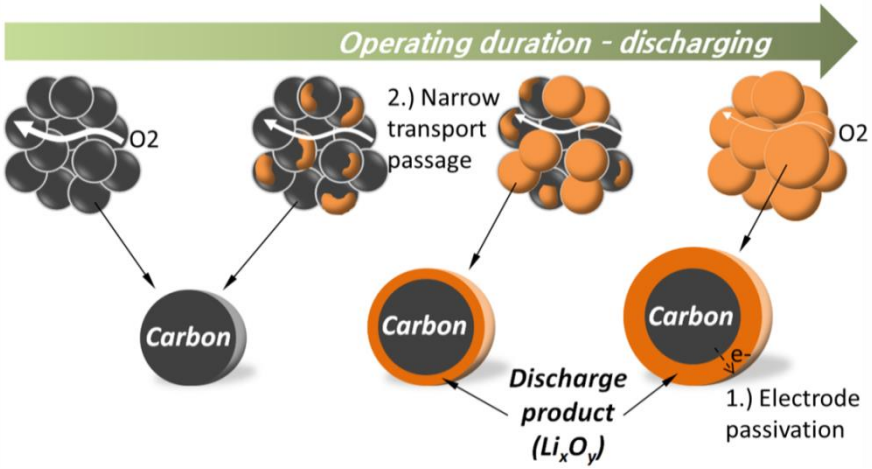
Typical growth modes of the oxide precipitate film in air cathodes. f.) the SEM image of precipitate on highly ordered pyrolytic graphite (HOPG) at 10 μA/cm^2 for 1M LiTriflate in DOL:DME (1:1 w/w)

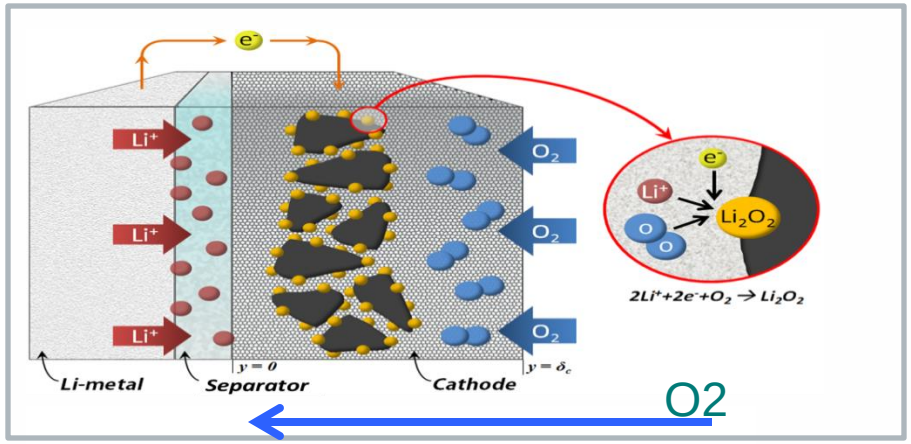
In practice, Surface coverage factor is determined by validating exp data

Y. Wang and S. C. Cho, Analysis of Air Cathode Performance for Lithium-air Batteries, Journal of The Electrochemical Society, 160 (10) A1-A9 (2013)

Voltage Losses

Porous electrodes





Oxygen profile

$$C_{O2}(y) = C_{O2,\delta} - \frac{I}{8F}\frac{\delta^2 - y^2}{\delta D_{O2}\left(\varepsilon_0 - \varepsilon_{prod}\right)^{\tau_d}} = C_{O2,\delta}\left[1 - Da\frac{1-(\frac{y}{\delta})^2}{\varepsilon_0^{\tau_d-\tau_{d,0}}\left(1-\frac{\varepsilon_{prod}}{\varepsilon_0}\right)^{\tau_d}}\right]$$

The Damköhler (Da) number:

$$Da = \frac{I}{8F}\frac{\delta}{C_{O2,\delta}\, D_{O2}\varepsilon_0^{\ \tau_{d,0}}} = \frac{\text{Reaction rate}}{\text{Mass transport rate}}$$

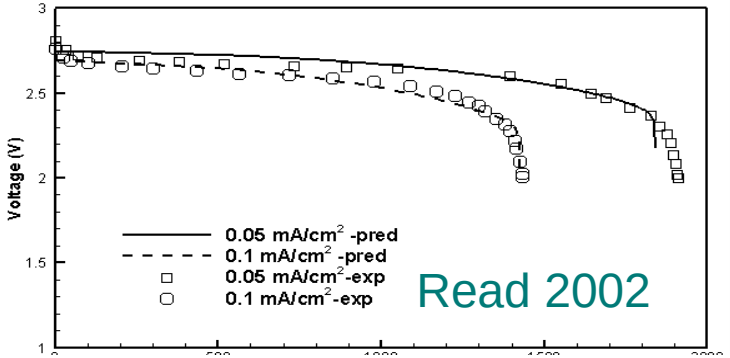
Overpotential

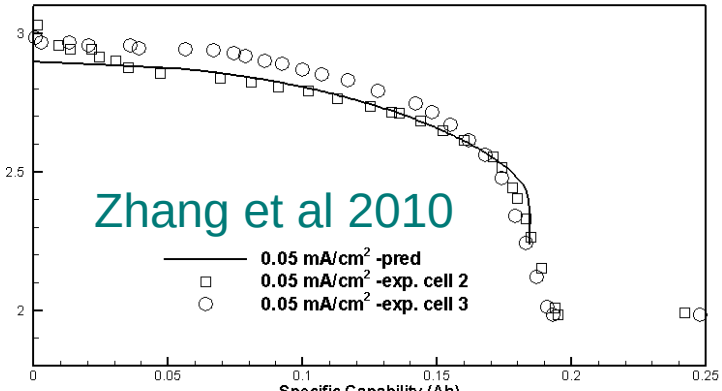
$$\Delta\eta = \frac{RT}{(1-\beta)F}\left(\tau_a \ln(1-\frac{\varepsilon_{prod}}{\varepsilon_0}) + (1-\beta)\ln\left(1 - Da\frac{1-(\frac{y}{\delta})^2}{\varepsilon_0^{\tau_d-\tau_{d,0}}(1-\frac{\varepsilon_{prod}}{\varepsilon_0})^{\tau_d}}\right)\right)$$

$$= \Delta\eta_a + \Delta\eta_{O2}$$

$$\Delta\eta = \Delta\eta_a + \Delta\eta_{O2}(y = \frac{\delta}{2})$$

Voltage Loss

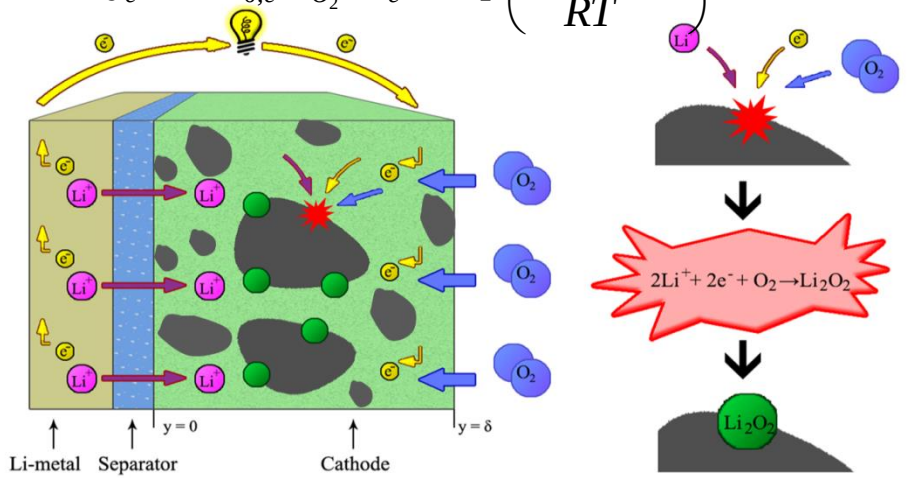




Y. Wang and S. C. Cho, Analysis of Air Cathode Performance for Lithium-air Batteries, Journal of The Electrochemical Society, 160 (10) A1-A9 (2013)

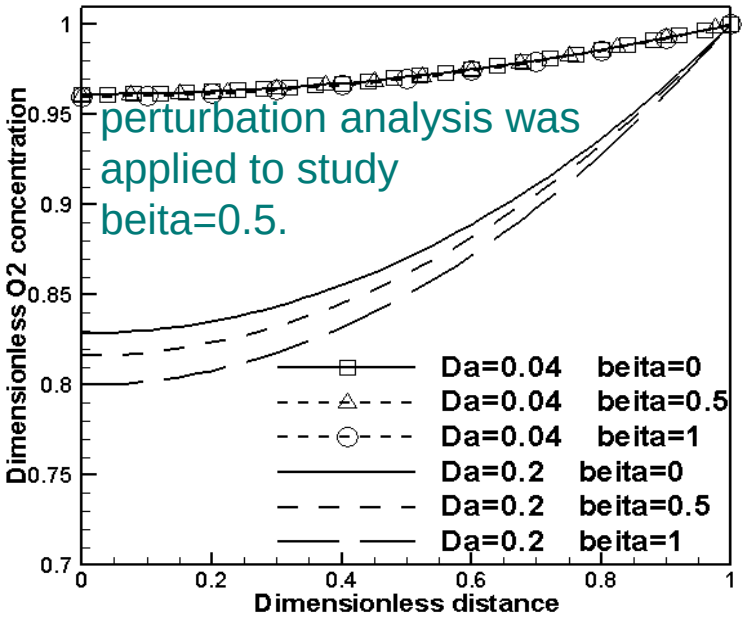
Oxygen Profiles

$$j_c = -ai_{0,c}^{ref} C_{O_2}^{1-\beta} C_e^{1-\beta} \exp\left(-\frac{\alpha}{RT} F\eta\right)$$



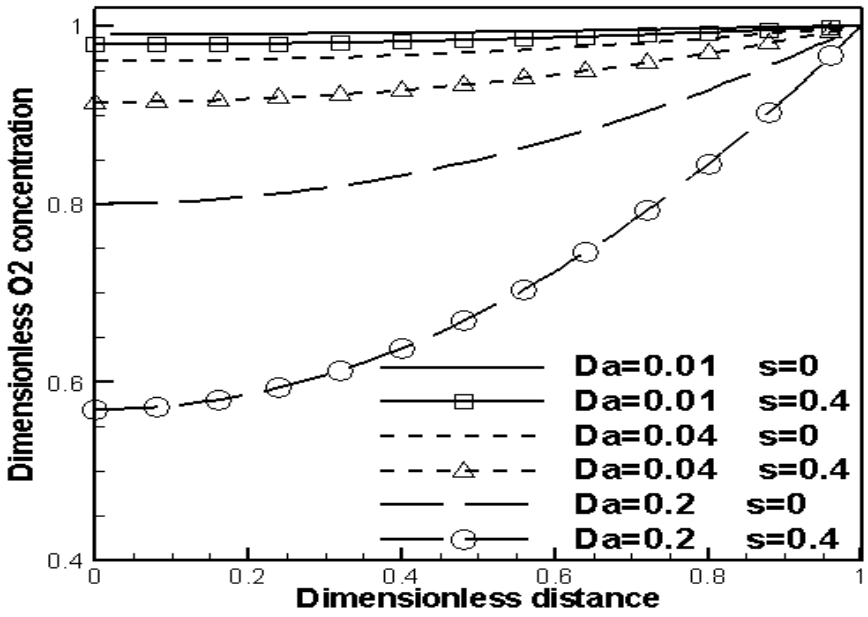
$$\bar{C}_{O2}(\bar{y}) = 1 - Da\frac{1-\bar{y}^2}{\varepsilon_0^{\tau_d-\tau_{d,0}}\left(1-\frac{\varepsilon_{prod}}{\varepsilon_0}\right)^{\tau_d}} = 1 - Da\frac{1-\bar{y}^2}{\varepsilon_0^{\tau_d-\tau_{d,0}}(1-s)^{\tau_d}}$$

$$Da = \frac{k\delta^2}{2D_{O2}^{eff} C_{O2,0}{}^{\beta}} = \frac{\text{Reaction rate}}{\text{Mass transport rate}}$$



perturbation analysis was applied to study beita=0.5.

Oxygen profiles in an air cathode under different Da and β.

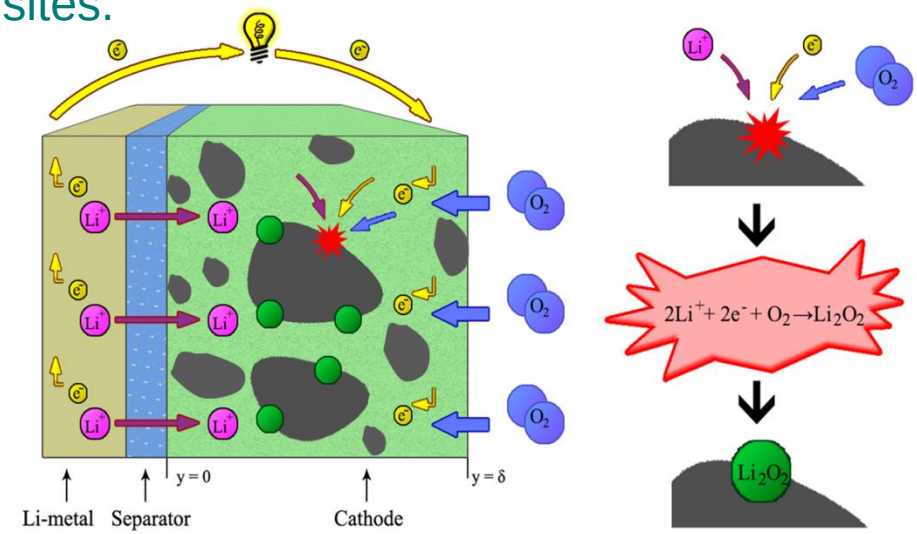


Oxygen profile in an air cathode under β=0.5 and two levels of the Li oxide volume fraction.

Y. Wang, Z. Wang, H. Yuan and T. Li, Discharge Oxide Storage Capacity And Voltage Loss In Li-air Battery, Electrochimica Acta, 180 (2015) 382-393

Li Oxide Storage Capacity: Smax

During discharging, insoluble Li oxides are produced and deposited at local reaction sites.



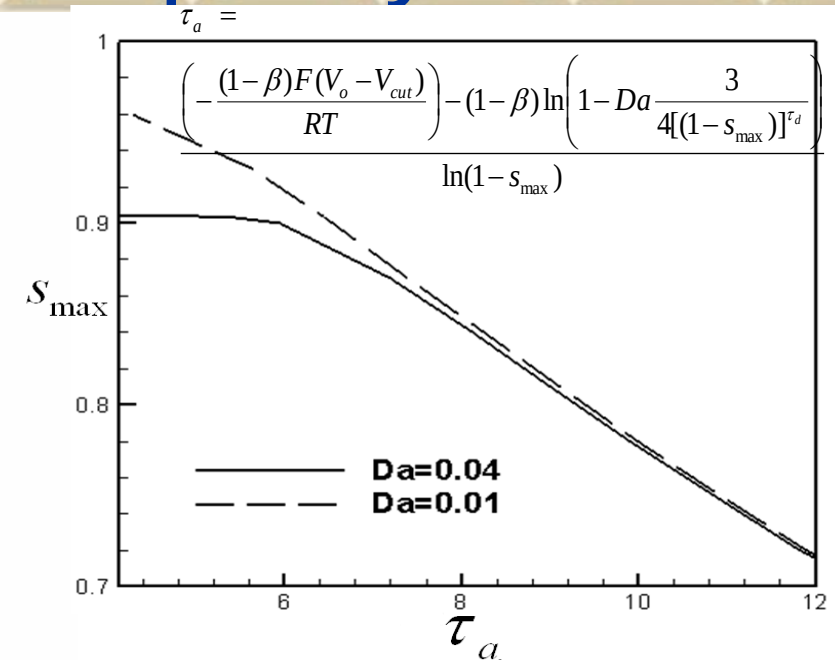
insoluble Li oxides' volume fraction

$$\varepsilon_{prod} = \int_0^t -\frac{j_c M_{prod}}{nF\rho_{prod}}\,dt = \varepsilon_{prod,0} + \frac{IM_{prod}}{n\delta F\rho_{prod}}\,t$$

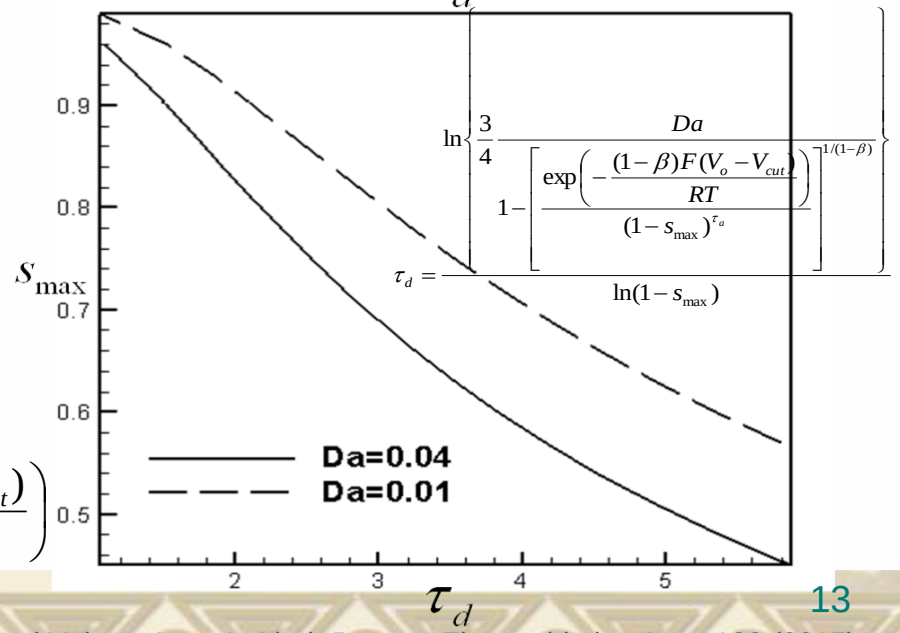
define $s = \dfrac{\varepsilon_{prod}}{\varepsilon_0}$

$$(1-s_{\max})^{\tau_a}\left(1-Da\frac{3}{4(1-s_{\max})^{\tau_d}}\right)^{1-\beta} = \exp\left(-\frac{(1-\beta)F(V_o-V_{cut})}{RT}\right)$$

$$\tau_a = \frac{\left(-\dfrac{(1-\beta)F(V_o-V_{cut})}{RT}\right)-(1-\beta)\ln\left(1-Da\dfrac{3}{4[(1-s_{\max})]^{\tau_d}}\right)}{\ln(1-s_{\max})}$$



$$\tau_d = \frac{\ln\left\{\dfrac{3}{4}\dfrac{Da}{1-\left[\dfrac{\exp\left(-\frac{(1-\beta)F(V_o-V_{cut})}{RT}\right)}{(1-s_{\max})^{\tau_a}}\right]^{1/(1-\beta)}}\right\}}{\ln(1-s_{\max})}$$

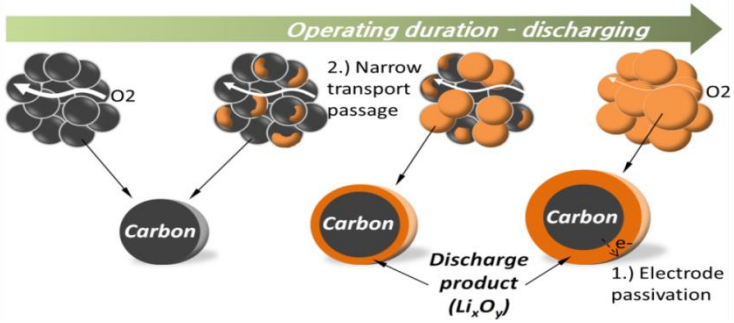


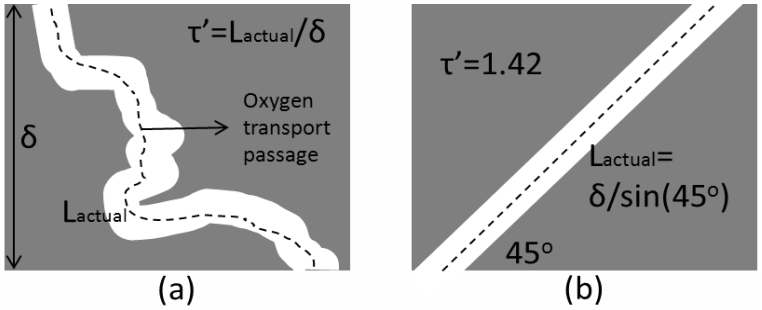
Y. Wang, Z. Wang, H. Yuan and T. Li, Discharge Oxide Storage Capacity And Voltage Loss In Li-air Battery, Electrochimica Acta, 180 (2015) 382-393

Morphology's Impacts on O2 Polarization

Oxygen related voltage loss:

$$\Delta\eta_{O2} = \frac{RT}{F}\ln\left(1 - Da\frac{1-(\frac{y}{\delta})^2}{\varepsilon_0^{\tau_d-\tau_{d,0}}(1-\frac{\varepsilon_{prod}}{\varepsilon_0})^{\tau_d}}\right)$$





MacMullin number (N_M) of a system consisting of a dispersed non-conducting phase in a conductive medium [29, 51].

Martínez et al. 2009

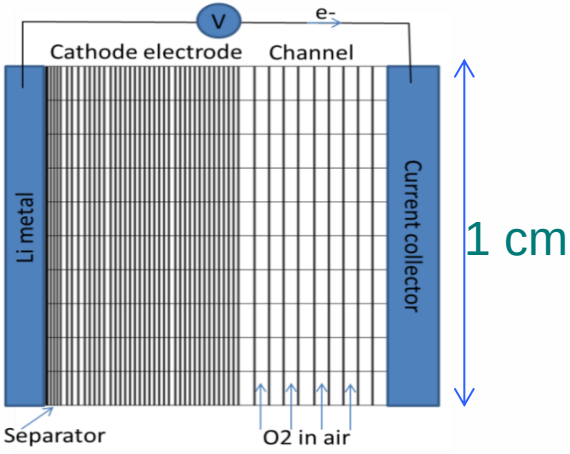
Label	Geometry	Arrangement	Size	Expression
I	Spheres	Random	Uniform	$N_M = \frac{(5-\varepsilon)(3+\varepsilon)}{8(1+\varepsilon)\varepsilon}$
II	Spheres	Cubic lattice	Uniform	$N_M = \frac{(3-\varepsilon)\left[\frac{4}{3}+0.409(1-\varepsilon)^{7/3}\right]-1.315(1-\varepsilon)^{10/3}}{2\varepsilon\left[\frac{4}{3}+0.409(1-\varepsilon)^{7/3}\right]-1.315(1-\varepsilon)^{10/3}}$
III	Spheres	Random and ordered	Range	$N_M = \varepsilon^{-1.5}$
IV	Cylinders	Parallel (square array)	Uniform	$N_M = \frac{2-\varepsilon-0.3058(1-\varepsilon)^4-1.334(1-\varepsilon)^8}{\varepsilon-0.3058(1-\varepsilon)^4-1.334(1-\varepsilon)^8}$
V	Fibrous material (Cylinders)	Random	-	$N_M = \frac{0.9126}{\varepsilon(\varepsilon-0.11)^{0.785}}$

$$Da = \frac{I}{8F}\frac{\delta}{C_{O2,\delta}D_{O2}\varepsilon_0^{\tau_{d,0}}} = \frac{\text{Reaction rate}}{\text{Mass transport rate}}$$

$$D_e^{eff} = \frac{D_e}{N_M}$$

Y. Wang and S. C. Cho, Analysis of Air Cathode Performance for Lithium-air Batteries, Journal of The Electrochemical Society, 160 (10) A1-A9 (2013)

Advanced Multi-dimensional Modeling



Conservation of Li ions

$$\frac{\partial \varepsilon C_e}{\partial t} = \nabla \cdot (D_e^{eff} \nabla C_e) + S_{Ce}$$

Conservation of species

$$\frac{\partial \varepsilon C_{O2,e}}{\partial t} = \nabla \cdot (D_{O2}^{eff} \nabla C_{O2,e}) + S_{O2}$$

Conservation of charges

$$0 = \nabla \cdot \left(\kappa^{eff} \nabla \Phi^{(e)} + \kappa_D^{eff} \nabla \ln C_e\right) + S_{\Phi^{(e)}}$$

$$0 = \nabla \cdot \left(\sigma^{eff} \nabla \Phi^{(s)}\right) + S_{\Phi^{(s)}}$$

Diffusional conductivity

$$\kappa_D^{eff} = \frac{2RT\kappa^{eff}}{F}(1-t_+^0)\left(1+\frac{d\ln f_{\pm}}{d\ln C_e}\right)$$

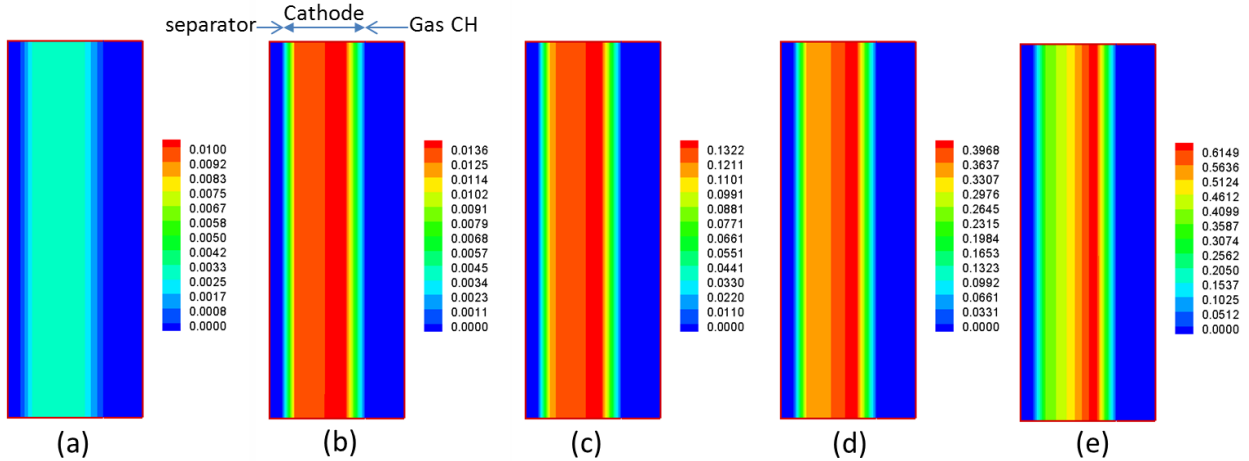
Electrochemical reaction rate (Tafel Equation)

$$j_c = -a\ (1-\frac{\varepsilon_{prod}}{\varepsilon})^{\tau_a} i_{0,c}^{ref} C_{O2}^{1-\beta} C_{Ce}^{1-\beta} \exp\left(-\frac{1-\beta}{RT} F\eta\right)$$

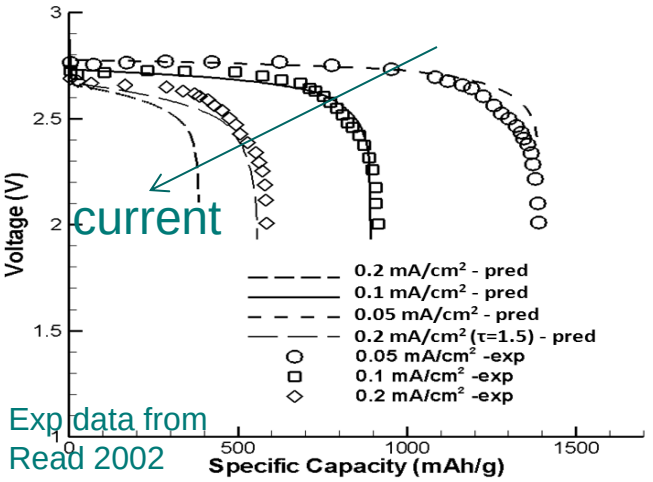
FVM $\nabla \cdot \vec{\Gamma}(\Theta) = S_\Theta$

$$B_p \Theta_p^n = \sum_m B_m \Theta_m^n + B(\Theta_p^0)$$

AMG



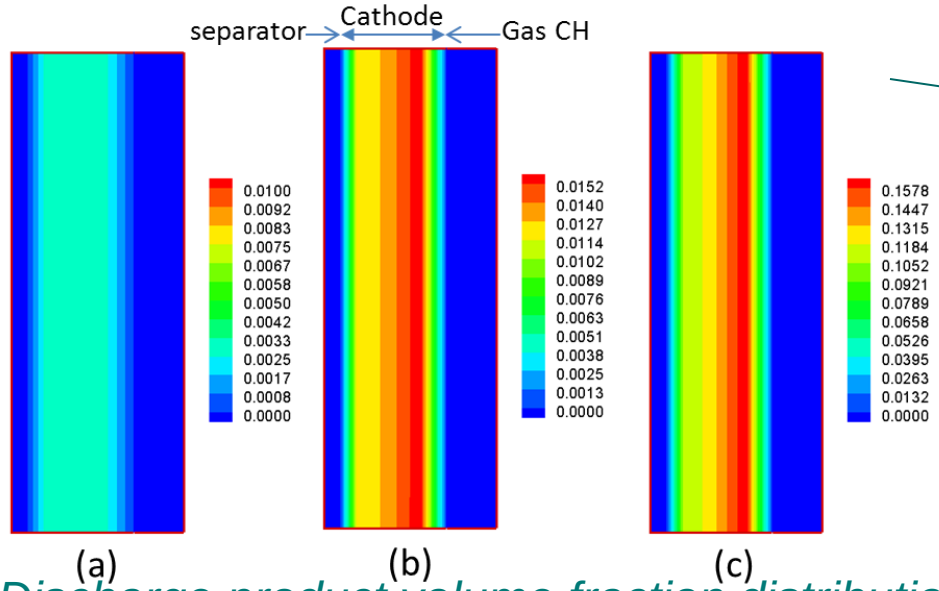
Discharge product volume fraction inside the cathode under 0.05 mA/cm²: (a)7.5 mAh/g; (b) 37.5 mAh/g; (c) 360 mAh/g; (d) 1080 mAh/g; (e) 1360 mAh/g.

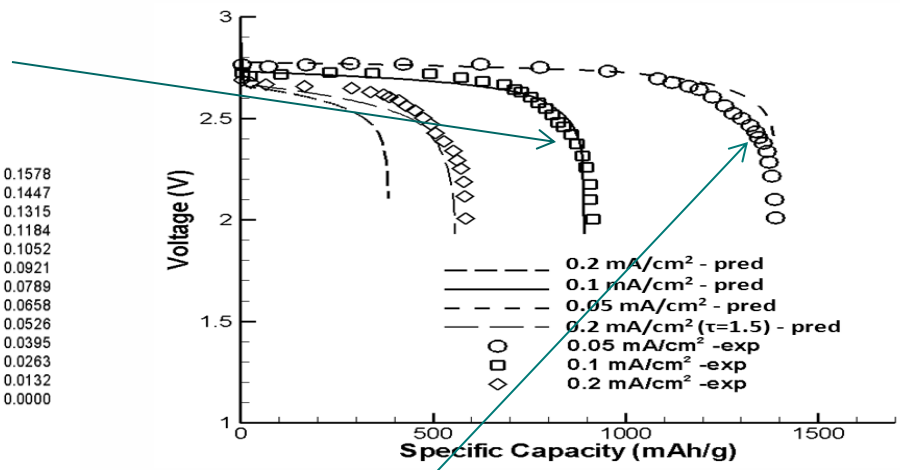


Exp data from Read 2002

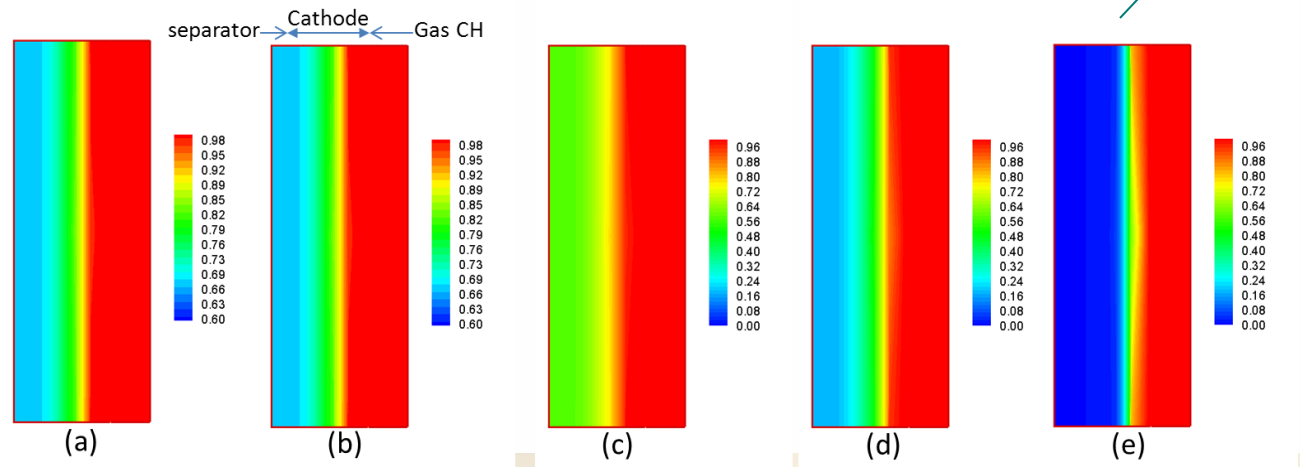
Y. Wang et al, Analysis and Three-dimensional Modeling of Vanadium Flow Batteries. Journal of The Electrochemical Society, 161(9), A1200-A1212

Advanced Multi-dimensional Modeling (II)





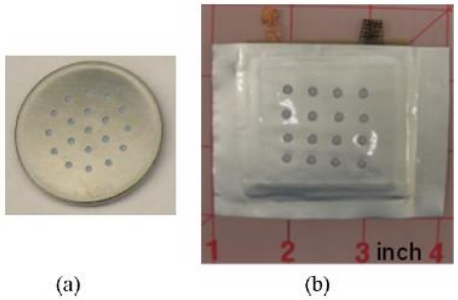
Discharge product volume fraction distributions inside the cathode electrode under 0.1 mA/cm^2: (a)7.5 mAh/g; (b) 37.5 mAh/g; (c) 360 mAh/g.



Dimensionless oxygen content inside the cathode electrode under 0.05 mA/cm^2: (a)7.5 mAh/g; (b) 37.5 mAh/g; (c) 360 mAh/g; (d) 1080 mAh/g; (e) 1360 mAh/g.

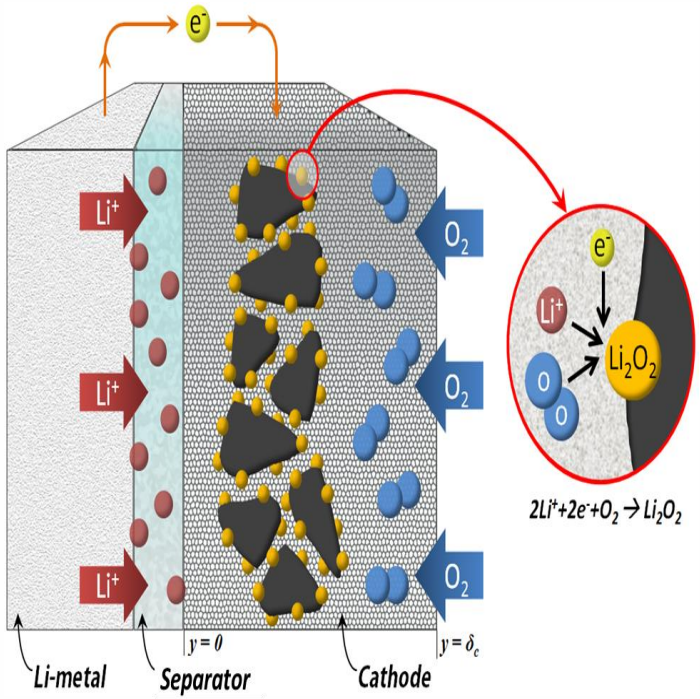
Y. Wang et al, Analysis and Three-dimensional Modeling of Vanadium Flow Batteries. Journal of The Electrochemical Society, 161(9), A1200-A1212

Towards High-Power Density Li-Air Battery



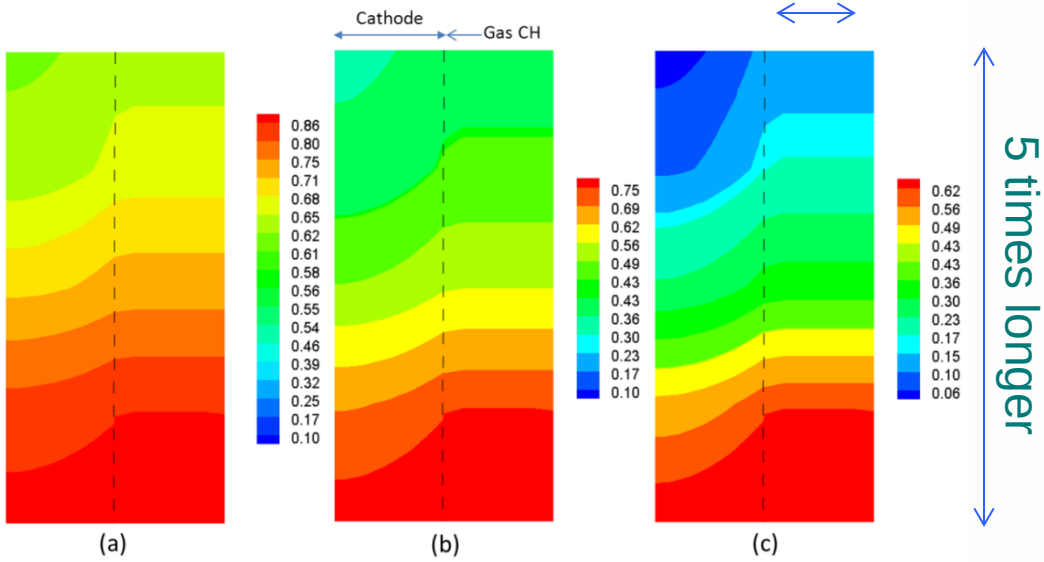
To reduce the volume of a Li-air battery and thus increase energy density, the gas channel dimension can be changed by increasing the aspect ratio of length to width, r.

Analytical solution $$\frac{C_{O2}-C_{O2}^{0}}{\frac{ILr}{4FD}}=\frac{x^{2}}{2L^{2}}-\frac{x}{L}$$





10 times less



5 times longer

Dimensionless oxygen in the cathode and gas channel under (a) 0.05 mA/cm², (b) 0.1 mA/cm², (c) 0.15 mA/cm² for a Li-air battery

Y. Wang et al, Analysis and Three-dimensional Modeling of Vanadium Flow Batteries. Journal of The Electrochemical Society, 161(9), A1200-A1212

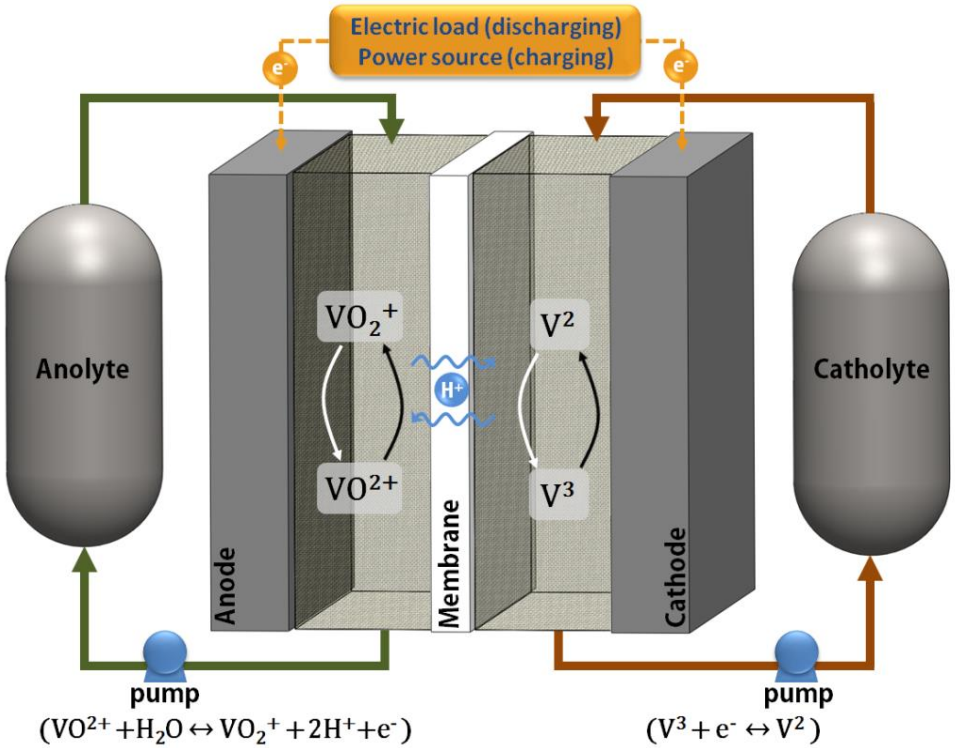
Other Ongoing Work: Vanadium Redox Flow Battery





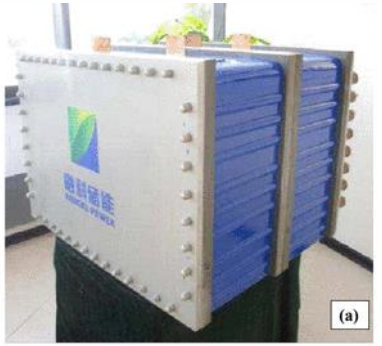
Intermittency of renewable energy needs energy storage solution

Flow battery technology offers several advantages in energy storage and conversion: 1.) almost unlimited capacity (related to tank volume); 2.) no degradation when left completely discharged for long periods; 3.) charge through electrolyte replacement or external power source; 4.) no permanent damage if the electrolytes are accidentally mixed.



Schematic of a flow battery (all vanadium redox flow battery as example)

Very similar to a Li-air or fuel cell system

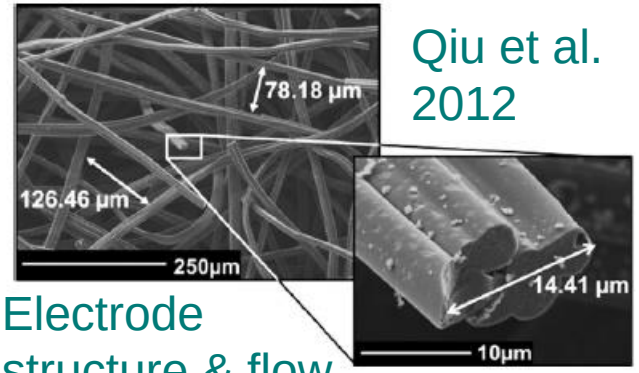


20kW VRB stack module developed by H. Zhang and co-workers at Dalian Institute of Chemical Physics and Dalian Rongke Power Co., Ltd



Innogy's 12 MW Regenesys plant at Little Barford, UK (1800 m3 of each electrolyte)

Other Ongoing Work: Advanced 3-D Modeling



Qiu et al. 2012

Electrode structure & flow

Fluid flow equations (continuity equation + Darcy's law)

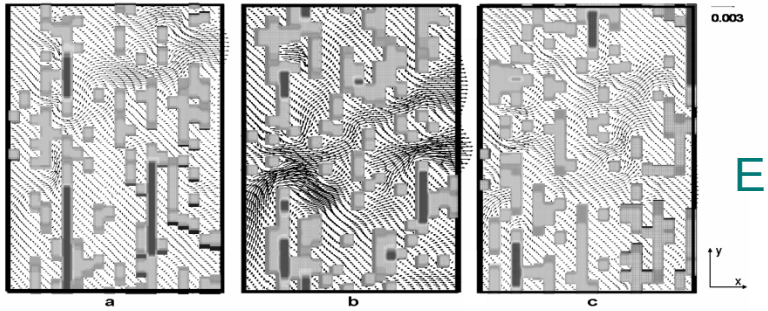
Conservation of species

$$\frac{\partial \varepsilon C_i}{\partial t} + \nabla \cdot (\vec{u} C_i) = \nabla \cdot (D_i^{eff} \nabla C_i + \frac{z_i C_i D_i^{eff}}{RT} F \nabla \Phi^{(e)}) + S_i$$

Conservation of charges

$$0 = \nabla \cdot \left(\kappa^{eff} \nabla \Phi^{(e)} + \kappa_D^{eff} \nabla \ln C_e \right) + S_{\Phi^{(e)}}$$

$$0 = \nabla \cdot \left(\sigma^{eff} \nabla \Phi^{(s)} \right) + S_{\Phi^{(s)}}$$

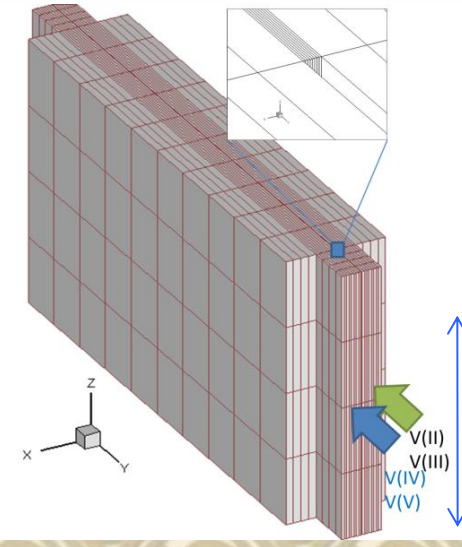


Diffusional conductivity

$$\kappa_D^{eff} = \frac{2RT\kappa^{eff}}{F}(1-t_+^0)\left(1+\frac{d\ln f_\pm}{d\ln C_e}\right)$$

Energy equation

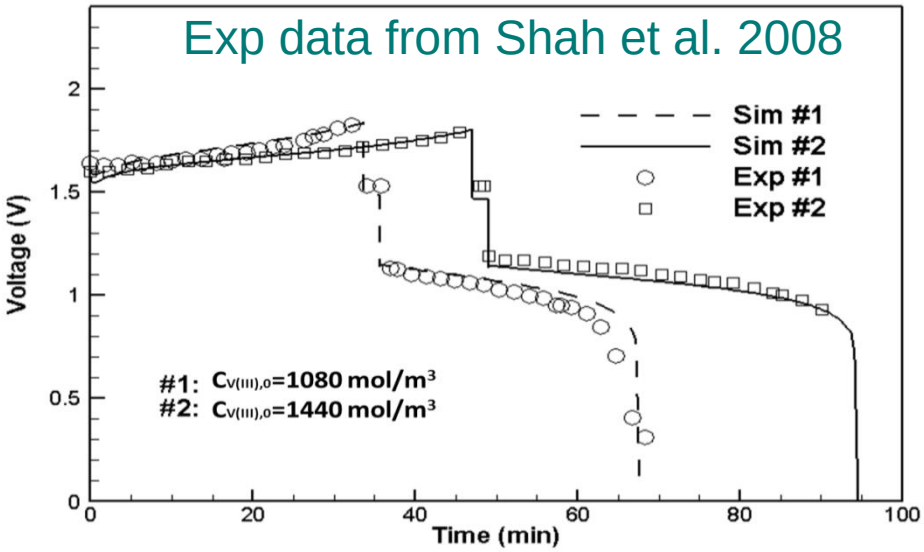
$$\frac{\partial}{\partial t}\left(\overline{\rho C_p} T\right) + \nabla \cdot \left(\vec{u}\rho_l C_{P,l} T\right) = \bar{\lambda}\nabla^2 T + S_T$$



3D Flow Battery computational domain

10 cm

Exp data from Shah et al. 2008



Conclusions

- Insoluble Li-oxides products greatly impact battery operation.
- The similarity between Li-air battery and PEM fuel cell was explained and stressed.
- A surface coverage model was proposed for Li-air battery to delineate insoluble Li-oxides formation and impacts;
- The oxygen transport and associated voltage loss were analyzed;
- Advanced multi-dimensional model was developed;
- Analysis and model were successfully validated against various experimental data;
- The multi-D simulation was developed for high-power Li-air battery design, which is currently under development in our lab.

Thanks!

Acknowledge:

1. NSF Energy for Sustainability support on travel under #1336873.
2. Dr. Jeff Read at US Army Research Lab for useful discussion.
3. The conference organizer for invitation.